

Echoes in brane worlds: ringing at a black hole–wormhole transition

Kirill A. Bronnikov^{1,2,3} and Roman A. Konoplya^{4,2,*}

¹*VNIIMS, Ozyornaya ul. 46, Moscow 119361, Russia*

²*Inst. of Gravitation and Cosmology, RUDN University,
ul. Miklukho-Maklaya 6, Moscow 117198, Russia*

³*National Research Nuclear University “MEPhI”, Kashirskoe sh. 31, Moscow 115409, Russia[†]*

⁴*Institute of Physics and Research Centre of Theoretical Physics and Astrophysics,
Faculty of Philosophy and Science, Silesian University in Opava, CZ-746 01 Opava, Czech Republic*

Echoes are known as modifications of the usual quasinormal ringing of a black hole at late times because of the deviation of space-time from the initial black-hole geometry in a small region near its event horizon. We consider a class of brane-world model solutions of the Shiromizu-Maeda-Sasaki equations, which describe both black holes and wormholes and interpolate between them via a continuous parameter. In this way the brane-world scenario provides a natural model for wormholes mimicking the black hole behavior if the continuous parameter is chosen near the threshold with a black-hole solution. We show that in the vicinity of this threshold interpolating between black holes and wormholes, quasinormal ringing of the wormholes at the initial stage is indistinguishable from that of the black holes with nearby values of the above parameter, but at later times the signal is modified by intensive echoes. We notice that the black-hole mimickers that are wormholes near the threshold have the largest quality factor and are therefore the best oscillators among the considered examples.

I. INTRODUCTION

Recent observations of black holes (BHs) and stars in the electromagnetic and gravitational channels [1–4] allow us to test the regime of strong gravity. Nevertheless, nowadays there is still large uncertainty in measuring the parameters of compact objects, such as their mass and angular momentum, which leaves considerable freedom for various interpretations of the geometries either towards BHs in modified theories of gravity or even in favor of such exotic objects as stable Schwarzschild stars or wormholes [5–11].

A wormhole geometry can be designed ad hoc in such a way that it would mimic the behavior of a BH in any astrophysically relevant processes (except for the Hawking radiation which is unlikely to be observed for large BHs) [5]. This is possible because the geometry of such a wormhole can be indistinguishable from that of the BH in the whole space outside a tiny region near the wormhole throat. At intermediately late times, classical radiation in the vicinity of a BH or wormhole must be dominated by the characteristic damped oscillations, quasinormal modes, which have been extensively studied [12–14] and were recently observed in, apparently, mergers of two BHs [1, 2].

While quasinormal modes of wormholes mimicking BHs are almost the same, the signal is modified at later times by echoes, what was first observed in [11] and further studied in a large number of papers (see, for example, [16–29] and references therein). In [11, 16] the echoes produced by various toy models of thin-shell wormholes were studied. A similar picture of echoes at the beginning

of the threshold between a regular BH and a wormhole has been found in [15] for the metric suggested in [30]. There, a continuous parameter of the metric allowed for interpolation between a regular BH, a one-way wormhole with an extremal null throat (the so called black bounce) and a traversable wormhole. However, the above wormhole metric is not a solution of any field equations and was simply designed ad hoc in the same manner as the Damour-Solodukhin wormhole [5] whose echoes were studied in [11].

A few examples of families of exact solutions containing both BHs and wormholes have been found with phantom scalar fields as sources of gravity (see, e.g., [31–34]), however, such solutions have been shown to be generically unstable under radial perturbations [34–37].

Here we will also consider various geometries interpolating between BHs and traversable wormholes via a continuous parameter, but which, unlike the previous models, are exact solutions of the Shiromizu-Maeda-Sasaki equations [38], describing the on-brane gravitational field in the second Randall-Sundrum brane-world scenario (RS2) [39]. The exact solutions to be studied concerning the possible echoes and quasinormal modes were obtained in [40, 41], and quasinormal modes in the frequency and time domains were studied in [44], but only for the range of parameters representing BHs. Thus the effect of echoes which should take place for wormholes in the parameter range near the threshold with BHs was missed in [44].

Having all the above motivations in mind, we would like to consider the quasinormal modes and ringing profiles for a few examples of the BH/wormhole solutions of the Shiromizu-Maeda-Sasaki equations in order to understand the possible general imprints of this extra-dimensional scenario on the ringing profile of BHs and wormholes, and especially at the transition between

* roman.konoplya@gmail.com

† kb20@yandex.ru

them. We will show that once the continuous parameter interpolating between the BH and wormhole solutions describes a wormhole near the “transition,” the quasinormal ringing is represented by damping oscillations appropriate for the near-threshold BH solution, but modified by echoes at later times. When the continuous parameter is further increased, then the echoes go over into the characteristic quasinormal ringing of the wormhole, while the period of the initial “threshold BH phase” damped oscillations diminishes and looks more like an initial outburst. The term “transition” must certainly be understood here with a considerable reservation: strictly speaking, we can only talk about values of this parameter making the geometry of a wormhole better or worse BH mimicker. Nevertheless, if one supposes that this parameter adiabatically changes with time as a result of some brane-world dynamic process, then the time-domain profiles of perturbations which relax at a much higher rate than the adiabatic change of the metric are qualitatively the same, as was shown, for example, in [61].

The paper is organized as follows. In Sec. II we briefly summarize the basic information about the brane-world model under consideration. Sec. III discusses the wave equations for test scalar and electromagnetic fields and the WKB and time-domain integration methods to be used for the analysis of ringing. Sec. IV is devoted to the quasinormal ringing of a few examples of BH and wormhole solutions with special emphasis to the parametric range near the transition between them. Finally, in the Conclusions we summarize the obtained results.

II. THE BRANE-WORLD MODEL

We will consider the second Randall-Sundrum brane-world model (RS2) [39] implying that our four-dimensional world is a hypersurface supporting all matter fields and embedded in a \mathbb{Z}_2 -symmetric five-dimensional spacetime (asymptotically AdS bulk), while the gravitational field propagates in the whole bulk. The gravitational field on the brane itself is described by the modified Einstein equations derived by Shiromizu, Maeda and Sasaki [38]

$$G_\mu^\nu = -\Lambda_4 \delta_\mu^\nu - \kappa_4^2 T_\mu^\nu - \kappa_5^4 \Pi_\mu^\nu - E_\mu^\nu, \quad (1)$$

where $G_\mu^\nu = R_\mu^\nu - \frac{1}{2} \delta_\mu^\nu R$ is the 4D Einstein tensor, Λ_4 is the 4D cosmological constant expressed in terms of the 5D cosmological constant Λ_5 and the brane tension λ :

$$\Lambda_4 = \frac{1}{2} \kappa_5^2 \left(\Lambda_5 + \frac{1}{6} \kappa_5^2 \lambda^2 \right); \quad (2)$$

$\kappa_4^2 = 8\pi G_N = \kappa_5^4 \lambda / (6\pi)$ is the 4D gravitational constant (G_N is the Newtonian constant of gravity); T_μ^ν is the stress-energy tensor of matter located on the brane; Π_μ^ν is a tensor quadratic in T_μ^ν , obtained from the matching conditions for the 5D metric across the brane:

$$\Pi_\mu^\nu = \frac{1}{4} T_\mu^\alpha T_\alpha^\nu - \frac{1}{2} T T_\mu^\nu - \frac{1}{8} \delta_\mu^\nu (T_{\alpha\beta} T^{\alpha\beta} - \frac{1}{3} T^2) \quad (3)$$

where $T = T^\alpha_\alpha$; lastly, E_μ^ν is the so-called “electric” part of the 5D Weyl tensor projected onto the brane: in proper 5D coordinates, we have $E_{\mu\nu} = \delta_\mu^A \delta_\nu^C {}^{(5)}C_{ABCD} n^B n^D$, where the capital letters A, B, \dots are 5D indices, and n^A is the unit normal vector to the brane. By construction, E_μ^μ is traceless, that is, $E_\mu^\mu = 0$ [38]. The general class and a number of particular examples describing wormholes and BHs in the above brane-world scenario were obtained in [40, 41].

A feature of utmost interest in these models is the generic appearance of families of solutions that unify symmetric wormholes and globally regular BHs with a minimum of the variable r (bounce) in their T-regions and a Kerr-like global structure. These two qualitatively different parts of any such family are separated by an extremal BH solution.

In what follows we will consider different examples of such solutions: one family representing the generic situation, another one with only an extremal BH, and the third one with a zero Schwarzschild mass. In each of these examples the metric is a vacuum solutions to Eqs. (1), with $T_\mu^\nu = 0$ and $\Lambda_4 = 0$; the effective energy-momentum tensor in the r.h.s. of (1) is thus the “tidal” tensor E_μ^ν of bulk origin. All metrics under consideration are asymptotically flat and have a zero Ricci scalar.

III. THE METHODS

Quasinormal modes of BHs are proper oscillations of BHs under specific boundary conditions, corresponding to purely outgoing waves at infinity and purely incoming waves at the event horizon (minus infinity in terms of the tortoise coordinate). The boundary conditions for a traversable wormhole which connects two infinities are the same in terms of the tortoise coordinate [45], so that many of the tools used for finding BH quasinormal modes can, with small modifications, be used for wormholes as well [37, 46, 47, 59, 60, 62, 63]. In particular, to finding the frequencies of quasinormal modes, we will use the WKB method when the effective potential has a single maximum and time domain integration for all types of the effective potentials.

A. Wave equations

The metric of a spherically symmetric static space-time can be written in the general form¹

$$ds^2 = -A(r)dt^2 + B(r)dr^2 + r^2(\sin^2 \theta d\phi^2 + d\theta^2). \quad (4)$$

¹ Note that we are using notations different from those in [41]: $B(r)$ of the present paper is equal to $1/B(r)$ of [41].

The generally covariant equation for a massless scalar field has the form

$$\frac{1}{\sqrt{-g}}\partial_\mu(\sqrt{-g}g^{\mu\nu}\partial_\nu\Phi) = 0 \quad (5)$$

and for an electromagnetic field

$$\frac{1}{\sqrt{-g}}\partial_\mu(F_{\rho\sigma}g^{\rho\nu}g^{\sigma\mu}\sqrt{-g}) = 0, \quad (6)$$

where $F_{\rho\sigma} = \partial_\rho A_\sigma - \partial_\sigma A_\rho$ and A_μ is the vector potential. After separation of variables, Eqs. (5) and (6) take the following general Schrödinger-like form:

$$\frac{d^2\Psi_s}{dr_*^2} + (\omega^2 - V(r))\Psi_s = 0, \quad (7)$$

where $s = 0$ corresponds to the scalar field and $s = 1$ to the electromagnetic field, the ‘‘tortoise coordinate’’ r_* is defined by the relation

$$dr_* = dr\sqrt{\frac{B(r)}{A(r)}}, \quad (8)$$

and the effective potentials are (see, e.g., Eq. (12a) in [54])

$$V_s(r) = A(r)\frac{\ell(\ell+1)}{r^2} + \frac{1}{2r}\frac{d}{dr}\frac{A(r)}{B(r)}, \quad (9)$$

$$V_{em}(r) = A(r)\frac{\ell(\ell+1)}{r^2}. \quad (10)$$

B. The WKB approach

For the analysis in the frequency domain we shall use the semi-analytical WKB method [48–52]. The essence of this approach is the expansion of the solution at both infinities in WKB series and matching these asymptotic expansions with the Taylor expansion near the peak of the effective potential. In addition, according to [50], we use a further representation of the WKB expansion in the form of the Padé approximants which, in most cases, greatly improves the accuracy of the WKB method. The WKB formula can be written in the following form [51]:

$$\begin{aligned} \omega^2 &= V_0 + A_2(\mathcal{K}^2) + A_4(\mathcal{K}^2) + A_6(\mathcal{K}^2) + \dots \\ &- i\mathcal{K}\sqrt{-2V_2}(1 + A_3(\mathcal{K}^2) + A_5(\mathcal{K}^2) + A_7(\mathcal{K}^2)\dots), \end{aligned} \quad (11)$$

where $\mathcal{K} = n + 1/2$, $n = 0, 1, 2, 3, \dots$

The corrections $A_k(\mathcal{K}^2)$ of order k to the eikonal formula are polynomials in \mathcal{K}^2 with rational coefficients and depend on the values V_2, V_3, \dots of higher-order derivatives of the potential $V(r)$ at its maximum. To increase accuracy of the WKB formula, we use the procedure suggested by Matyjasek and Opala [50], which consists in using the Padé approximants. For the order k of the

WKB formula (11) we define a polynomial $P_k(\epsilon)$ in the following way

$$\begin{aligned} P_k(\epsilon) &= V_0 + A_2(\mathcal{K}^2)\epsilon^2 + A_4(\mathcal{K}^2)\epsilon^4 + A_6(\mathcal{K}^2)\epsilon^6 + \dots \\ &- i\mathcal{K}\sqrt{-2V_2}(\epsilon + A_3(\mathcal{K}^2)\epsilon^3 + A_5(\mathcal{K}^2)\epsilon^5 \dots), \end{aligned} \quad (12)$$

and the squared frequency is obtained for $\epsilon = 1$:

$$\omega^2 = P_k(1).$$

For the polynomial $P_k(\epsilon)$ we will use Padé approximants

$$P_{\tilde{n}/\tilde{m}}(\epsilon) = \frac{Q_0 + Q_1\epsilon + \dots + Q_{\tilde{n}}\epsilon^{\tilde{n}}}{R_0 + R_1\epsilon + \dots + R_{\tilde{m}}\epsilon^{\tilde{m}}}, \quad (13)$$

with $\tilde{n} + \tilde{m} = k$, such that, near $\epsilon = 0$,

$$P_{\tilde{n}/\tilde{m}}(\epsilon) - P_k(\epsilon) = \mathcal{O}(\epsilon^{k+1}).$$

Usually, for finding the fundamental mode ($n = 0$) frequency, Padé approximants with $\tilde{n} \approx \tilde{m}$ provide the best approximation. In [50], $P_{6/6}(1)$ and $P_{6/7}(1)$ were compared to the 6th-order WKB formula $P_{6/0}(1)$. In [51] it has been observed that usually even $P_{3/3}(1)$, i. e. a Padé approximation of the 6th-order gives a more accurate value for the squared frequency than $P_{6/0}(1)$. Here we will use the 7th WKB expansions with $\tilde{m} = 3$ Padé approximation and show that the results obtained at different WKB orders are in a very good agreement.

C. Time-domain integration

We will integrate the wavelike equations rewritten in terms of the light-cone variables $u = t - r_*$ and $v = t + r_*$. The appropriate discretization scheme was suggested in [53]:

$$\begin{aligned} \Psi(N) &= \Psi(W) + \Psi(E) - \Psi(S) \\ &- \Delta^2 \frac{V(W)\Psi(W) + V(E)\Psi(E)}{8} + \mathcal{O}(\Delta^4), \end{aligned} \quad (14)$$

where we use the following designations for the points: $N = (u + \Delta, v + \Delta)$, $W = (u + \Delta, v)$, $E = (u, v + \Delta)$ and $S = (u, v)$. The initial data are specified on the null surfaces $u = u_0$ and $v = v_0$. To extract the values of the quasinormal frequencies, we will use the Prony method which allows us to fit the signal by a sum of exponentials with some excitation factors.

IV. THE PICTURE OF QUASINORMAL RINGING FOR VARIOUS SOLUTIONS

A. The Casadio-Fabbri-Mazzacurati (CFM) metric

Our first example with the Schwarzschild generating function $A(r) = 1 - 2M/r$ [41] represents the generic behavior of brane-world BH/wormhole families. The metric

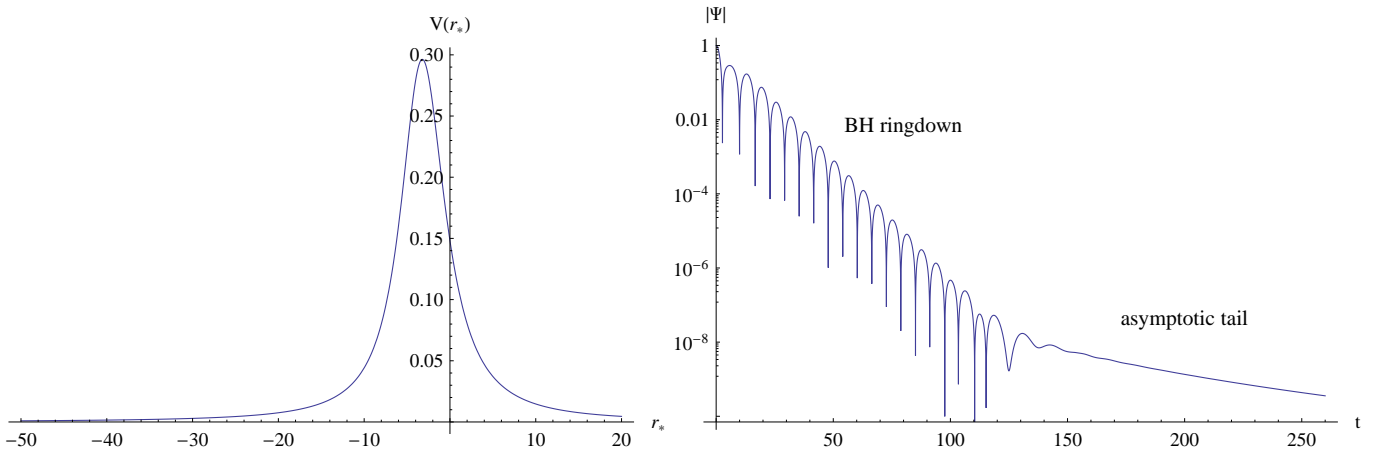


FIG. 1. The effective potential (left) and the semi-logarithmic plot of the time-domain profile (right) for perturbations of the electromagnetic field in the vicinity of the double horizon of CFM BHs with the metric 15 where $r_0 = 2M$, $M = 1/2$, $\ell = 1$. The quasinormal ringing goes over into asymptotic power-law tails.

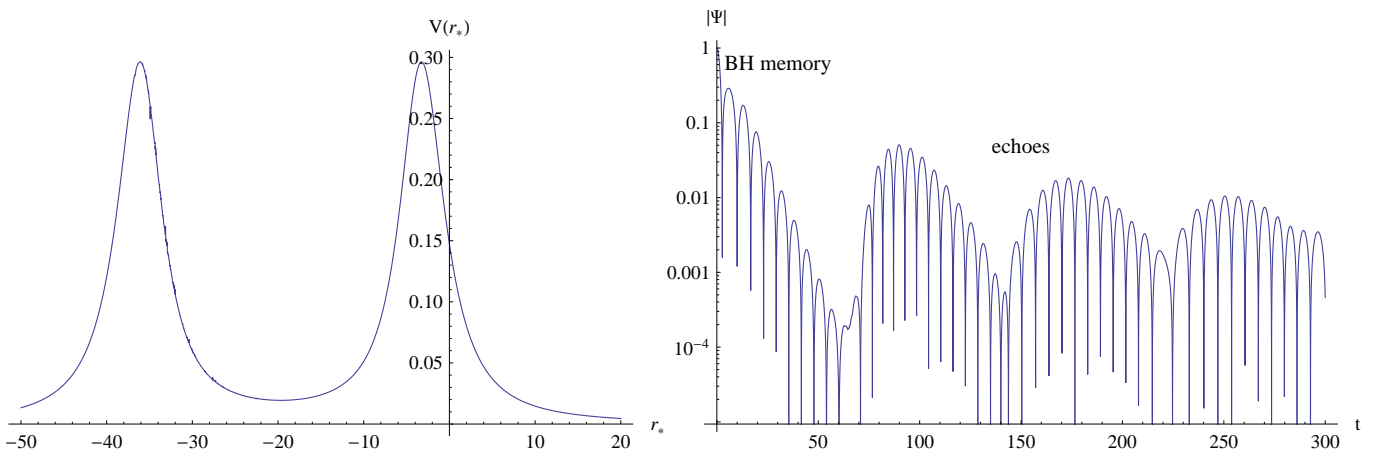


FIG. 2. The effective potential (left) and the semi-logarithmic plot of the time-domain profile (right) for perturbations of the electromagnetic field in the vicinity of a CFM wormhole with $M = 1/2$, $r_0 = 1.01$, $\ell = 1$. The first long period of damped oscillations is indistinguishable from that of the threshold BH metric (that corresponds to $r_0 = 2M$), but, at later times it goes over into a series of echoes.

has the form

$$ds^2 = \left(1 - \frac{2M}{r}\right) dt^2 - \frac{1 - 3M/(2r)}{(1 - 2M/r)(1 - r_0/r)} dr^2 - r^2 d\Omega^2. \quad (15)$$

The Schwarzschild metric is reproduced in the special case $r_0 = 3M/2$. The metric (15) has been obtained by Casadio, Fabbri and Mazzacurati [42] in search for new brane-world BH solutions and by Germani and Maartens [43] as a possible metric outside a homogeneous star on the brane.

In the case $r_0 > 2M$, the metric (15) describes a symmetric traversable wormhole [40].

In the intermediate case $r_0 = 2M$ we obtain a BH with a double horizon at $r = 2M$.

In the case $r_0 < 2M$, there is a BH with a sin-

gle horizon at $r = 2M$. As described in Ref. [42], the global space-time structure depends on the sign of $\eta = r_0 - 3M/2$. If $\eta < 0$, this structure coincides with that of a Schwarzschild BH, but the spacelike curvature singularity is located at $r = 3M/2$ instead of $r = 0$. If $\eta > 0$, the solution describes a nonsingular BH with a minimum value of the variable r equal to $r_0 > 3M/2$ inside the horizon, that is, a bounce in the two angular directions of a Kantowski-Sachs anisotropic cosmology.

In Fig. 1 one can see the usual picture of evolution of perturbations in the vicinity of a BH, now for the threshold case $r_0 = 2M$. It consists of the initial outburst which changes into damped quasinormal oscillations and power-law asymptotic tails in the end. Figure 2 shows perturbations of a wormhole corresponding to $r_0 = 2.02M$, that is, very close to the threshold with the BH state, and there emerges a distinctive picture of echoes after the initial os-

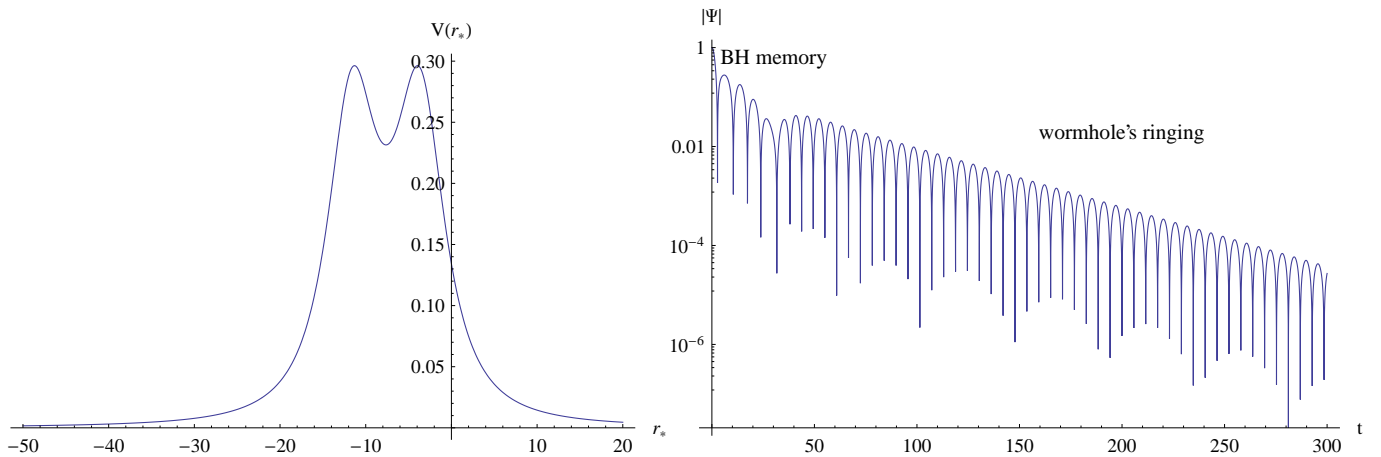


FIG. 3. The effective potential (left) and the semi-logarithmic plot of the time-domain profile (right) for perturbations of the electromagnetic field in the vicinity of a CFM wormhole with $M = 1/2$, $r_0 = 1.2$, $\ell = 1$. The first relatively short period of damped oscillations is a kind of memory of the threshold BH state $r_0 = 2M$, and it goes over into the characteristic quasinormal mode of the wormhole at later times.

TABLE I. Quasinormal mode frequencies ω of the electromagnetic field for $\ell = 1$ in the CFM metric.¹⁵

r_0	Time-domain	WKB
0	$0.43751 - 0.24617i$	$0.43782 - 0.24904i$
0.2	$0.45313 - 0.23549i$	$0.45365 - 0.23682i$
0.4	$0.46936 - 0.22148i$	$0.46942 - 0.22174i$
0.6	$0.48557 - 0.20288i$	$0.48509 - 0.20306i$
0.75	$0.49653 - 0.18495i$	$0.49652 - 0.18498i$
0.8	$0.49983 - 0.17789i$	$0.50056 - 0.17729i$
1	$0.50651 - 0.14686i$	$0.50652 - 0.14733i$
1.1	$0.50177 - 0.11188i$, echoes	–
1.2	$0.48143 - 0.06821i, 0.99460 - 0.00979i$	–
1.3	$0.47713 - 0.07202i, 0.56376 - 0.04650i$	–
10	initial outburst, $0.12759 - 0.03054i$	–
20	initial outburst, $0.06552 - 0.01498i$	–

cillatory fall-off corresponding to the residual fundamental mode of the boundary $r_0 = 2M$ BH. Finally, when the parameter r_0 is further increased, the echoes go over into the established characteristic quasinormal ringing of a wormhole (Fig. 3).

Table I exhibits the dominant quasinormal frequencies of the CFM metric in both regimes. In the BH case $r_0 \leq 2M$, the quasinormal modes can be computed with both time-domain integration and WKB methods. Near the threshold, when $r_0 \gtrsim 2M$, the WKB formula, implying two turning points, cannot be used since the effective potential has two barriers and four turning points.

We can see that for BHs the results produced by the WKB method and time-domain integration are in a very good concordance, with disagreement always less than one percent. Taking into account that the extraction of frequencies from the profiles obtained with the help of time-domain integration greatly depends on the temporal range which is determined as the “quasinormal ring-

ing,” a relative error within one percent can be easily ascribed not even to the WKB formula but rather to the arbitrariness of the period of quasinormal ringing. Here we used the 7th order WKB formula with the further Padé approximants such that $\tilde{m} = 3$, which gives the best agreement with the results of time-domain integration for the Schwarzschild case $r_0 = 3/(2M)$ and also coincides (within a 5-digits accuracy) with the accurate numerical value $0.49652 - 0.18498i$. For the case of a wormhole very close to the threshold, we have only a single mode which is the residual or, in a sense, “memory” of the boundary BH solution. The echoes which follow this residual mode cannot be represented by a single dominant quasinormal mode. Nevertheless, when the parameter r_0 is further increased, the enveloping oscillations of echoes (visible in Fig. 2) align, and the characteristic mode of the wormhole establishes, being reflected in the second frequency given in Table 1. We can also see that at $r_0 \gg 2M$ the real and imaginary parts of the frequency are inversely

TABLE II. Quasinormal modes of the electromagnetic field for $\ell = 1$ for the BK-1 metric 16.

r_0	Time-domain	WKB
1	$0.53569 - 0.06300i$	$0.53569 - 0.06299i$
1.1	$0.53360 - 0.06227i$, echoes	–
1.2	$0.51232 - 0.05364i$, echoes	–
1.3	$0.50762 - 0.04834i$, echoes	–
1.4	$0.49793 - 0.04302i, 0.55835 - 0.01965i$	–
1.5	$0.47806 - 0.03107i, 0.55859 - 0.02937i$	–

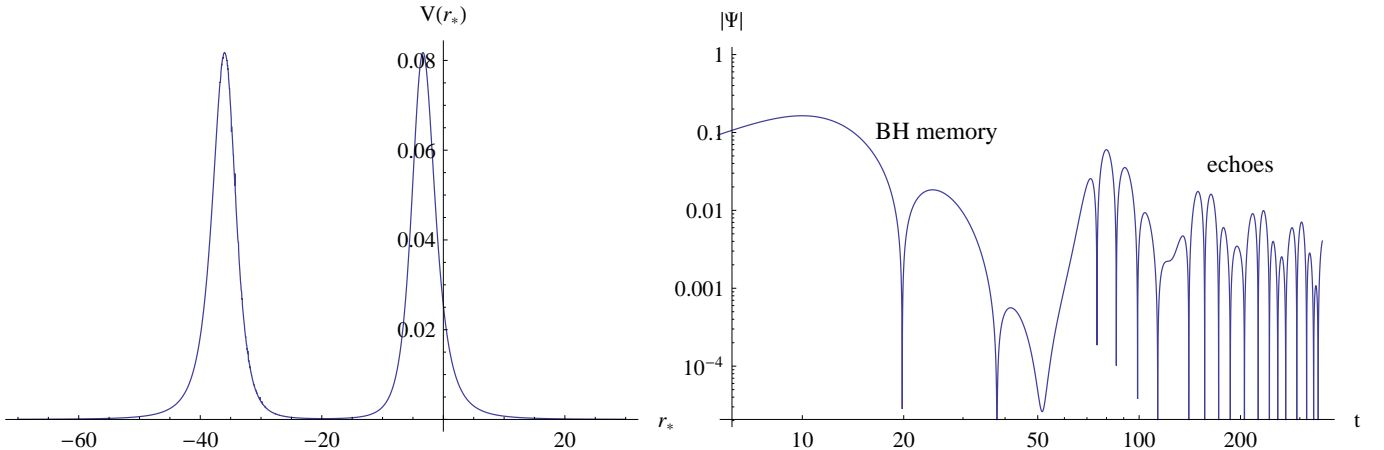


FIG. 4. The effective potential (left) and the logarithmic plot of the time-domain profile (right) for perturbations of the scalar field in the vicinity of the CFM wormhole with $M = 1/2$, $r_0 = 1.01$, $\ell = 0$. Several first oscillations (usual for $\ell = 0$ perturbations) are indistinguishable from those of the threshold BH metric (corresponding to $r_0 = 2M$), but at later times they go over into a series of echoes.

proportional to r_0 .

The above description concerned the behavior of electromagnetic perturbations against the background of brane-world BHs and wormholes. It can be verified that massless scalar field perturbations show similar qualitative features, as can be seen in Fig. 4 that depicts the behavior of radial scalar perturbations ($\ell = 0$) of a CFM wormhole.

B. The Bronnikov-Kim-1 (BK-1) metric

This case represents an atypical example of a BH-wormhole family of solutions. The metric can be written as

$$ds^2 = \left(1 - \frac{2M}{r}\right)^2 dt^2 - \left(1 - \frac{r_0}{r}\right)^{-1} \left(1 - \frac{r_1}{r}\right)^{-1} dr^2 - r^2 d\Omega^2, \quad r_1 := \frac{Mr_0}{r_0 - M}, \quad (16)$$

The only BH solution corresponds to the case $r_0 = r_1 = 2M$, which coincides with the extremal Reissner-Nordström metric.

Other values of r_0 lead either to wormholes (the throat is located at $r = r_0$ if $r_0 > 2M$ or at $r = r_1 > 2M$ in

case $2M > r_0 > M$), or to a naked singularity located at $r = 2M$ (if $r_0 < M$) (see more details in Ref. [40]).

Figure 5 shows the picture of evolution of perturbation in the vicinity of the threshold, which is qualitatively the same as for the previous metric, with a distinction related to the length of the initial (residual) quasinormal ringing which is much longer now, and also the frequencies change slower with changing r_0 . This picture simply reflects the fact that larger r_0 are necessary to deviate from the threshold BH geometry $r_0 = 2M$ at the same extent.

C. The Bronnikov-Kim-2 (BK-2) metric

This example differs from the previous ones by having a zero value of the Schwarzschild mass of the brane-world BHs and wormholes. The metric is

$$ds^2 = \left(1 - \frac{h^2}{r^2}\right) dt^2 - \left(1 - \frac{h^2}{r^2}\right)^{-1} \left(1 + \frac{C - h}{\sqrt{2r^2 - h^2}}\right)^{-1} dr^2 - r^2 d\Omega^2 \quad (17)$$

The sphere $r = h$ is a simple horizon if $C > 0$ and a double horizon if $C = 0$. In the case $C < 0$, $B(r)$ has a

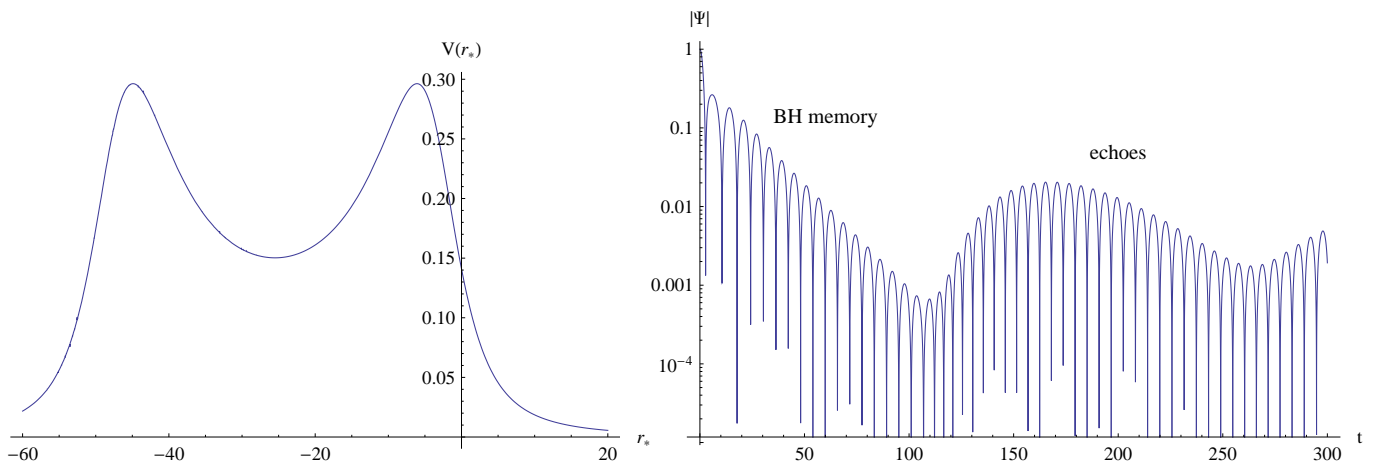


FIG. 5. The effective potential (left) and the semi-logarithmic plot of the time-domain profile (right) for perturbations of the electromagnetic field in the vicinity of the BK-1 wormhole: $M = 1/2$, $r_0 = 1.1$, $\ell = 1$. The first long period of damped oscillations is indistinguishable from that of the threshold BH metric (that corresponds to $r_0 = 2M$), but at later times emerges a series of echoes.

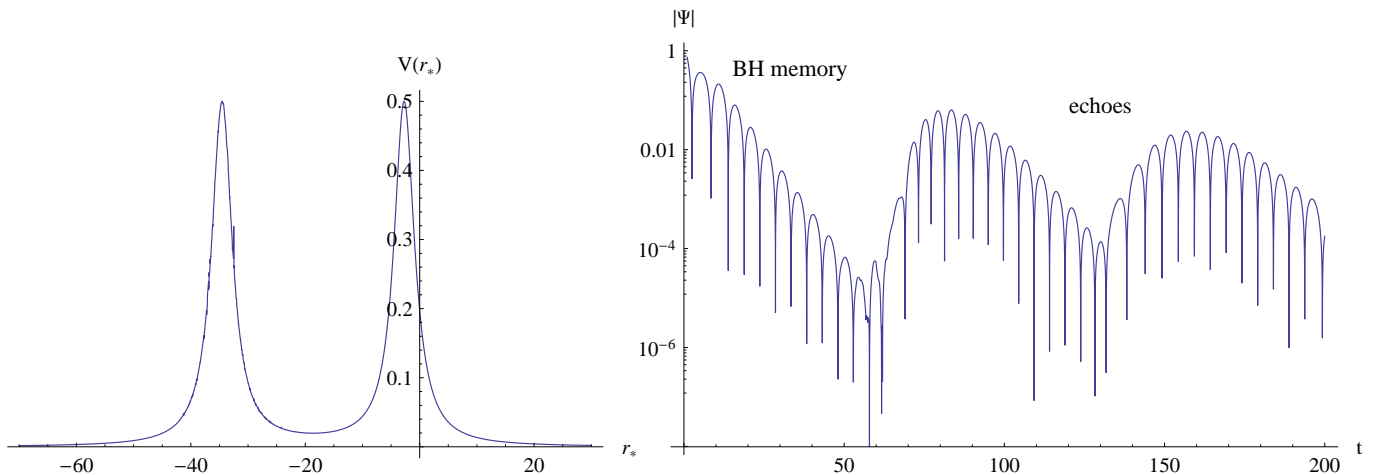


FIG. 6. The effective potential (left) and the semi-logarithmic plot of the time-domain profile (right) for perturbations of the electromagnetic field in the vicinity of the BK-2 wormhole 17 with $M = 1/2$, $C = -0.01$, $\ell = 1$. The first long period of damped oscillations is indistinguishable from that of the threshold BH metric (corresponding to $C = 0$), but at later times it goes over into a series of echoes.

TABLE III. Quasinormal modes of the electromagnetic field for $\ell = 1$ in the BK-2 metric 17.

C	Time-domain	WKB
1.5	$0.53695 - 0.34301i$	$0.54096 - 0.33905i$
1	$0.57668 - 0.31754i$	$0.57663 - 0.31785i$
0.5	$0.61726 - 0.27547i$	$0.61983 - 0.27457i$
0.1	$0.64156 - 0.22399i$	$0.64144 - 0.22379i$
0	$0.64439 - 0.20921i$	$0.64435 - 0.20900i$
-0.01	$0.64306 - 0.20529i$, echoes	—
-0.1	$0.61509 - 0.09685i$, echoes	—
-0.3	$0.59897 - 0.07043i$, $0.70323 - 0.03991i$	—
-0.5	initial outburst, $0.73833 - 0.07600i$	—
-0.7	initial outburst, $0.73338 - 0.09961i$	—

simple zero at $r = r_{\text{th}} > h$ given by

$$2r_{\text{th}}^2 = h^2 + (h - C)^2, \quad (18)$$

which is a symmetric wormhole throat [40].

The evolution of perturbations in this example is qualitatively similar to the two previous cases: the echoes appears immediately after the threshold, providing wormholes mimicking the BH behavior. If we consider the quality factor of the mode, which is proportional to the ratio of the real oscillations frequency to the damping rate,

$$Q \sim \frac{\text{Re}(\omega)}{|\text{Im}(\omega)|},$$

we can see that oscillations of BHs have a maximum quality factor in the extremal state at the threshold. This is true not only for the last example but for all models under consideration. Moreover, if one considers wormholes with the parameter C (or r_0 in the previous examples) near the threshold, one can see that the quality factor continues growing and starts to decrease only when echoes are damped. This is also a common feature of all three examples.

V. CONCLUSIONS

We have used the higher-order WKB method with Padé approximants [48–52] and time-domain integration [53] in order to analyze the quasinormal ringing of BH and wormhole solutions in the RS2 brane-world model. The metrics under consideration depend on a continuous parameter interpolating between BHs and wormholes, so that if the parameter is larger than some threshold value, then the BH “goes over” into a wormhole. We have shown that this “transition” from BHs to wormholes near the threshold is characterized by echoes: the

first stage of damped oscillations, representing the memory of the threshold BH state is accompanied by a series of echoes at later times. When the same parameter is further increased, the echoes damp and pass on into the characteristic ringing of the wormhole.

This picture is observed for all examples considered here and, apparently, does not depend on the particular model. We believe that this kind of behavior should not depend on the spin of the field as well and should be valid not only for the scalar and electromagnetic fields considered here, but also for the gravitational field because the echoes are induced by appearing of the second symmetric peak in the far left region (in terms of the tortoise coordinate), producing the second scattering and partial reflection of the signal at late times.

Although the characteristic dominant quasinormal frequency of the BHs and wormholes under consideration can behave differently in different examples, there is one feature observed in all the considered models. The ratio of the real oscillation frequency to the damping rate, which is proportional to the quality factor of oscillations, always decreases as the BH solution moves away from the threshold. On the other hand, the quality factor continues increasing on the other side of the threshold for wormholes which still mimic the BH behavior, that is, for the residual mode. In other words, wormholes near the threshold are the best oscillators among all the considered examples. Therefore, it is not excluded that this monotonic behavior of the quasinormal frequency might be a more general property of the brane-world models.

ACKNOWLEDGMENTS

The authors acknowledge the support of the grant 19-03950S of Czech Science Foundation (*GAČR*). The work of K.B. was partly performed within the framework of the Center FRPP supported by MPhI Academic Excellence Project (contract No. 02.a03.21.0005, 27.08.2013).

The work was also funded by the RUDN University Program 5-100 and by the RFBR grant No. 19-02-00346.

-
- [1] B. P. Abbott *et al.* [LIGO Scientific and Virgo Collaborations], *Phys. Rev. Lett.* **116**, no. 6, 061102 (2016) [arXiv:1602.03837 [gr-qc]].
 - [2] B. P. Abbott *et al.* [LIGO Scientific and Virgo Collaborations], *Phys. Rev. Lett.* **116**, no. 22, 221101 (2016) [arXiv:1602.03841 [gr-qc]].
 - [3] C. Goddi *et al.*, *Int. J. Mod. Phys. D* **26**, no. 02, 1730001 (2016) [arXiv:1606.08879 [astro-ph.HE]].
 - [4] K. Akiyama *et al.* [Event Horizon Telescope Collaboration], *Astrophys. J.* **875**, no. 1, L1 (2019).
 - [5] T. Damour and S. N. Solodukhin, *Phys. Rev. D* **76**, 024016 (2007); [arXiv:0704.2667 [gr-qc]].
 - [6] R. Konoplya and A. Zhidenko, *Phys. Lett. B* **756**, 350 (2016) [arXiv:1801.03587 [gr-qc]].
 - [7] R. A. Konoplya, C. Posada, Z. Stuchlík and A. Zhidenko, *Phys. Rev. D* **100**, no. 4, 044027 (2019) [arXiv:1905.08097 [gr-qc]].
 - [8] C. Posada and C. Chirenti, *Class. Quant. Grav.* **36**, 065004 (2019) [arXiv:1811.09589 [gr-qc]].
 - [9] S. W. Wei and Y. X. Liu, *Phys. Rev. D* **98**, no. 2, 024042 (2018) [arXiv:1803.09530 [gr-qc]].
 - [10] E. Berti, K. Yagi, H. Yang and N. Yunes, *Gen. Rel. Grav.* **50**, no. 5, 49 (2018) [arXiv:1602.04738 [gr-qc]].
 - [11] V. Cardoso, E. Franzin and P. Pani, *Phys. Rev. Lett.* **116**, no. 17, 171101 (2016) Erratum: [*Phys. Rev. Lett.* **117**, no. 8, 089902 (2016)] [arXiv:1602.07309 [gr-qc]].

- [12] R. A. Konoplya and A. Zhidenko, *Rev. Mod. Phys.* **83**, 793 (2011) [arXiv:1102.4014 [gr-qc]].
- [13] K. D. Kokkotas and B. G. Schmidt, *Living Rev. Rel.* **2** (1999) 2 [gr-qc/9909058].
- [14] E. Berti, V. Cardoso and A. O. Starinets, *Class. Quant. Grav.* **26**, 163001 (2009) [arXiv:0905.2975 [gr-qc]].
- [15] M. S. Churilova and Z. Stuchlik, arXiv:1911.11823 [gr-qc].
- [16] V. Cardoso, S. Hopper, C. F. B. Macedo, C. Palenzuela and P. Pani, *Phys. Rev. D* **94**, no. 8, 084031 (2016) [arXiv:1608.08637 [gr-qc]].
- [17] V. Cardoso and P. Pani, *Nat. Astron.* **1**, no. 9, 586 (2017) [arXiv:1709.01525 [gr-qc]].
- [18] K. W. Tsang *et al.*, *Phys. Rev. D* **98**, no. 2, 024023 (2018) [arXiv:1804.04877 [gr-qc]].
- [19] R. A. Konoplya, Z. Stuchlik and A. Zhidenko, *Phys. Rev. D* **99**, no. 2, 024007 (2019) [arXiv:1810.01295 [gr-qc]].
- [20] E. Barausse, V. Cardoso and P. Pani, *Phys. Rev. D* **89**, no. 10, 104059 (2014) [arXiv:1404.7149 [gr-qc]].
- [21] H. Nakano, N. Sago, H. Tagoshi and T. Tanaka, *PTEP* **2017**, no. 7, 071E01 (2017) [arXiv:1704.07175 [gr-qc]].
- [22] A. Testa and P. Pani, *Phys. Rev. D* **98**, no. 4, 044018 (2018) [arXiv:1806.04253 [gr-qc]].
- [23] M. Mirbabayi, arXiv:1807.04843 [gr-qc].
- [24] Y. T. Wang, Z. P. Li, J. Zhang, S. Y. Zhou and Y. S. Piao, *Eur. Phys. J. C* **78**, no. 6, 482 (2018) [arXiv:1802.02003 [gr-qc]].
- [25] P. Bueno, P. A. Cano, F. Goelen, T. Hertog and B. Vernocke, *Phys. Rev. D* **97**, no. 2, 024040 (2018) [arXiv:1711.00391 [gr-qc]].
- [26] A. Maselli, S. H. Volkel and K. D. Kokkotas, *Phys. Rev. D* **96**, no. 6, 064045 (2017) [arXiv:1708.02217 [gr-qc]].
- [27] Z. P. Li and Y. S. Piao, *Phys. Rev. D* **100**, no. 4, 044023 (2019) [arXiv:1904.05652 [gr-qc]].
- [28] Y. T. Wang, J. Zhang, S. Y. Zhou and Y. S. Piao, *Eur. Phys. J. C* **79**, no. 9, 726 (2019) [arXiv:1904.00212 [gr-qc]].
- [29] V. Cardoso, V. F. Foit and M. Kleban, *JCAP* **1908**, 006 (2019) doi:10.1088/1475-7516/2019/08/006 [arXiv:1902.10164 [hep-th]].
- [30] A. Simpson and M. Visser, *JCAP* **1902**, 042 (2019) [arXiv:1812.07114 [gr-qc]].
- [31] K. A. Bronnikov and J. C. Fabris, *Phys. Rev. Lett.* **96**, 251101 (2006); gr-qc/0511109.
- [32] K. A. Bronnikov, V. N. Melnikov and H. Dehnen, *Gen. Rel. Grav.* **39**, 973–987 (2007); gr-qc/0611022
- [33] S. V. Bolokhov, K. A. Bronnikov, and M. V. Skvortsova, *Class. Quantum Grav.* **29**, 245006 (2012); arXiv:1208.4619.
- [34] K. A. Bronnikov, *Particles* **2018**, 1, 5; arXiv: 1802.00098.
- [35] J. A. Gonzalez, F. S. Guzman and O. Sarbach, *Class. Quantum Grav.* **26**, 015010 (2009).
- [36] K. A. Bronnikov, J. C. Fabris and A. Zhidenko, *Eur. Phys. J. C* **71** (11), 1791 (2011); ArXiv: 1109.6576.
- [37] K. A. Bronnikov, R. A. Konoplya and A. Zhidenko, *Phys. Rev. D* **86**, 024028 (2012) [arXiv:1205.2224 [gr-qc]]
- [38] T. Shiromizu, K. Maeda and M. Sasaki, *Phys. Rev. D* **62** 024012 (2000).
- [39] L. Randall and R. Sundrum, *Phys. Rev. Lett.* **83**, 4690 (1999), hep-ph/9906064.
- [40] K. A. Bronnikov and S.-W. Kim, *Phys. Rev. D* **67**, 064027 (2003) [gr-qc/0212112].
- [41] K. A. Bronnikov, V. N. Melnikov and H. Dehnen, *Phys. Rev. D* **68**, 024025 (2003) [gr-qc/0304068].
- [42] R. Casadio, A. Fabbri and L. Mazzacurati, *Phys. Rev. D* **65**, 084040 (2001); gr-qc/0111072.
- [43] C. Germani and R. Maartens, *Phys. Rev. D* **64**, 124010 (2001); hep-th/0107011.
- [44] E. Abdalla, B. Cuadros-Melgar, A. B. Pavan and C. Molina, *Nucl. Phys. B* **752**, 40 (2006) [gr-qc/0604033].
- [45] R. A. Konoplya and C. Molina, *Phys. Rev. D* **71**, 124009 (2005) [gr-qc/0504139].
- [46] R. A. Konoplya and A. Zhidenko, *JCAP* **1612**, 043 (2016) [arXiv:1606.00517 [gr-qc]].
- [47] R. A. Konoplya and A. Zhidenko, *Phys. Rev. D* **81**, 124036 (2010) [arXiv:1004.1284 [hep-th]].
- [48] B. F. Schutz and C. M. Will, *Astrophys. J.* **291**, L33 (1985).
- [49] S. Iyer and C. M. Will, *Phys. Rev. D* **35**, 3621 (1987).
- [50] J. Matyjasek and M. Opala, *Phys. Rev. D* **96**, no. 2, 024011 (2017) [arXiv:1704.00361 [gr-qc]].
- [51] R. A. Konoplya, A. Zhidenko and A. F. Zinhailo, *Class. Quant. Grav.* **36**, 155002 (2019) [arXiv:1904.10333 [gr-qc]].
- [52] R. A. Konoplya, *Phys. Rev. D* **68**, 024018 (2003) [gr-qc/0303052].
- [53] C. Gundlach, R. H. Price and J. Pullin, *Phys. Rev. D* **49**, 883 (1994) [gr-qc/9307009].
- [54] A. F. Zinhailo, *Eur. Phys. J. C* **78**, no. 12, 992 (2018) [arXiv:1809.03913 [gr-qc]].
- [55] P. D. Roy, S. Aneesh and S. Kar, arXiv:1910.08746 [gr-qc].
- [56] A. Ovgun, I. Sakalli and H. Mutuk, arXiv:1904.09509 [gr-qc].
- [57] R. Oliveira, D. M. Dantas, V. Santos and C. A. S. Almeida, *Class. Quant. Grav.* **36**, no. 10, 105013 (2019) [arXiv:1812.01798 [gr-qc]].
- [58] J. L. Blázquez-Salcedo, X. Y. Chew and J. Kunz, *Phys. Rev. D* **98**, no. 4, 044035 (2018) [arXiv:1806.03282 [gr-qc]].
- [59] R. A. Konoplya, *Phys. Lett. B* **784**, 43 (2018) [arXiv:1805.04718 [gr-qc]].
- [60] S. Aneesh, S. Bose and S. Kar, *Phys. Rev. D* **97**, no. 12, 124004 (2018) [arXiv:1803.10204 [gr-qc]].
- [61] E. Abdalla, C. B. M. H. Chirenti and A. Saa, *Phys. Rev. D* **74**, 084029 (2006) doi:10.1103/PhysRevD.74.084029 [gr-qc/0609036].
- [62] M. S. Churilova, R. A. Konoplya and A. Zhidenko, arXiv:1911.05246 [gr-qc].
- [63] M. A. Cuyubamba, R. A. Konoplya and A. Zhidenko, *Phys. Rev. D* **98**, no. 4, 044040 (2018) [arXiv:1804.11170 [gr-qc]].